HHS Public Access

Author manuscript

J Inherit Metab Dis. Author manuscript; available in PMC 2024 November 01.

Published in final edited form as:

J Inherit Metab Dis. 2023 November ; 46(6): 1147–1158. doi:10.1002/jimd.12660.

CRISPR/Cas9-based double strand oligonucleotide insertion strategy corrects metabolic abnormalities in murine glycogen storage disease type Ia

Ananya Samanta[1], **Nelson George**[1], **Irina Arnaoutova**[1], **Hung-Dar Chen**[1], **Brian C. Mansfield**[1], **Christopher Hart**[2], **Troy Carlo**[2], **Janice Y. Chou**[1,*]

[1]Section on Cellular Differentiation, Division of Translational Medicine, *Eunice Kennedy Shriver* National Institute of Child Health and Human Development, National Institutes of Health, Bethesda, MD 20892, USA,

[2]Current affiliation, Prime Medicine Inc, Cambridge, MA 02139, USA.

Abstract

Glycogen storage disease type-Ia (GSD-Ia), characterized by impaired blood glucose homeostasis, is caused by a deficiency in glucose-6-phosphatase-α (G6Pase-α or G6PC). Using the *G6pc*-R83C mouse model of GSD-Ia, we explored a CRISPR/Cas9-based double-strand DNA oligonucleotide (dsODN) insertional strategy that uses the non-homologous end joining repair mechanism to correct the pathogenic p.R83C variant in *G6pc* exon-2. The strategy is based on the insertion of a short dsODN into *G6pc* exon-2 to disrupt the native exon, and to introduce an additional splice acceptor site and the correcting sequence. When transcribed and spliced the edited gene would generate a wild-type mRNA encoding the native G6Pase-α protein. The editing reagents formulated in lipid nanoparticles (LNP) were delivered to the liver. Mice were treated either with one dose of LNP-dsODN at age 4 weeks or with 2 doses of LNP-dsODN at age 2 and 4 weeks. The *G6pc*-R83C mice receiving successful editing expressed ~4% of normal hepatic G6Pase-α activity, maintained glucose homeostasis, lacked hypoglycemic seizures, and displayed normalized blood metabolite profile. The outcomes are consistent with preclinical studies supporting previous gene augmentation therapy which is currently in clinical trials. This editing strategy may offer the

*Correspondence should be addressed to: Janice Y. Chou, Building 10, Room 8N-240C, NIH, 10 Center Drive, Bethesda, MD 20892-1830, Tel: 301-496-1094; Fax: 301-402-6035, chouja@mail.nih.gov.

AUTHOR CONTRIBUTIONS

Ananya Samanta performed the experiments, analyzed the data and wrote the paper; Nelson George, Irina Arnaoutova, and Hung-Dar Chen performed the experiments, analyzed the data, and edited the manuscript; Christopher Hart and Troy Carlo designed the LNP-dsODN reagents, analyzed the data, and edited the manuscript; Brian C. Mansfield analyzed the data and edited the manuscript; Janice Y. Chou designed the research, acquired the funding, analyzed the data, wrote the paper, and is the GUARANTOR for the article.

CONFLICT OF INTEREST

Ananya Samanta, Nelson George, Irina Arnaoutova, Hung-Dar Chen, Brian C. Mansfield, and Janice Y. Chou declare that they have no conflicts of interest.

Christopher Hart and Troy Carlo are former employees of CRISPR Therapeutics, Inc., and own shares of CRISPR Therapeutics stock.

INFORMED CONSENT

This article does not contain any studies with human subjects performed by any of the authors.

ANIMAL RIGHTS

All institutional and national guidelines for the care and use of laboratory animals were followed.

basis for a therapeutic approach with an earlier clinical intervention than gene augmentation, with the additional benefit of a potentially permanent correction of the GSD-Ia phenotype.

Keywords

Glucose-6-phosphatase-α; genome editing; glycogen storage disease type Ia mouse model; lipid nanoparticles; non-homologous end joining

1 | INTRODUCTION

Type Ia glycogen storage disease (GSD-Ia; MIM232200) is an autosomal recessive disorder caused by pathogenic variants in glucose-6-phosphatase-α (G6Pase-α or G6PC) that is expressed primarily in the liver, kidney, and intestine.[1–3] G6Pase-α catalyzes the hydrolysis of glucose-6-phosphate (G6P) to glucose and phosphate and GSD-Ia patients manifest a phenotype of impaired glucose homeostasis characterized by fasting hypoglycemia, hepatomegaly, nephromegaly, hyperlipidemia, hyperuricemia, lactic acidemia, and growth retardation.[1–3] GSD-Ia can be neonatal lethal, without intervention to stabilize blood glucose levels. The current dietary therapies[4–6] have enabled GSD-Ia patients to maintain a normalized metabolic phenotype, if adhered to strictly, but compliance is challenging. Moreover, dietary therapies do not correct the underlying pathological processes in GSD-I patients. Consequently, hepatocellular adenoma/carcinoma (HCA/HCC), which are severe long-term complications, still occur in metabolically compensated GSD-I patients.[1–3,7]

We have developed a recombinant adeno-associated virus (rAAV) vector-mediated gene augmentation therapy for GSD-Ia,[8–10] which, licensed to Ultragenyx Pharmaceutical (Novato, CA), is now in a phase III clinical trial (NCT05139316). For a pediatric disease, a rAAV-based gene augmentation therapy might have a restricted window of therapeutic intervention until liver growth has slowed sufficiently to retain a therapeutic dose of the episomal rAAV-*G6PC* vector.[8] Currently, there is insufficient clinical data to understand if multi-decade episomal transgene expression can be maintained in the human liver at a therapeutic level,[11] especially considering a recent report on the rate of physiological liver cell replacement.[12] Extended durability is important for a pediatric disease. We therefore explored alternative genetic technologies for GSD-Ia therapy, such as CRISPR/Cas9-based gene editing.[13–18] We previously generated a *G6pc*-R83C mouse strain[19] carrying the prevalent pathogenic G6PC-p.R83C variant[20,21] and showed that the *G6pc*-R83C mice exhibit the pathophysiology of impaired glucose homeostasis mimicking human GSD-Ia.[19] In an initial exploration of CRISP/Cas-9-based editing using AAV to deliver the CRISPR reagents, we showed that a homology directed repair (HDR) strategy could correct the abnormal metabolic phenotype of neonatal *G6pc*-R83C mice.[19]

Mammalian cells use two major repair pathways for DNA double-strand break (DSB), HDR that is restricted to the S and G2 phases of the cell cycle and non-homologous end joining (NHEJ) which is active throughout the cell cycle, and the major pathway for DSB repair in both dividing and non-dividing cells.[22–24] We therefore explore a CRISPR/Cas9-based short double-stranded DNA oligonucleotide (dsODN) insertional strategy[25] utilizing NHEJ to improve editing efficiency and expand the therapeutic window for intervention. To reduce

any risk associated with AAV delivery and the resulting extended expression of the editing reagents, we delivered the reagents transiently, formulated as lipid nanoparticles (LNP).[26,27]

In this study, we evaluated the efficacy of the dsODN insertional strategy[25] to treat 2- to 4-week-old *G6pc*-R83C mice. We have previously shown that GSD-Ia mice expressing ≥3% of normal hepatic G6Pase-α activity maintain glucose homeostasis.[9,10, 19] We now show that the dsODN insertional strategy restored hepatic G6Pase-α activity to ~4% of normal hepatic activity in the *G6pc*-R83C mice and increased the 0% survival rate to age 6 weeks for the untreated *G6pc*-R83C mice to a 100% survival rate to age 16 weeks for the dsODN-treated mice. Furthermore, the LNP-dsODN-treated mice could maintain glucose homeostasis and sustain long hours of fasting. Taken together, the dsODN insertional strategy may offer a permanent, non-inheritable, liver cell genome correction.

2 | MATERIALS AND METHODS

2.1 | Animals

All animal studies were conducted under an animal protocol approved by the *Eunice Kennedy Shriver* National Institute of Child Health and Human Development Animal Care and Use Committee. The *G6pc*-R83C mice carrying a prevalent human pathogenic G6PC-p.R83C variant manifest a phenotype of impaired glucose homeostasis mimicking human GSD-Ia with a 6-week-survival rate of 0%.[19] Consequently, we used the *G6pc*-R83 (wild-type) and *G6pc*-R83/R83C (heterozygote) mice with indistinguishable phenotype as controls.[19] Mice were maintained on a standard NIH-31 Open formula mouse/rat sterilizable diet from Envigo (Madison, WI). To sustain the survival of the untreated *G6pc*-R83C mice beyond age 1 week, a glucose therapy consisting of daily subcutaneous injection of 100–150 μl of 15% glucose per mouse starting at age 8 days. For the LNP-dsODN infused mice, glucose therapy was terminated immediately after infusion. Liver samples from control and LNP-dsODN-treated mice were collected at sacrifice without fasting.

2.2 | The dsODN insertional strategy and phenotype analysis

CRISPR Therapeutics supplied the LNP formulated with Cas9 mRNA, the single-strand *G6pc* exon 2-specific guide RNA (gRNA), and the correcting *G6pc* exon 2-specific dsODN. The gRNA spacer sequence UGGACAAUGCCCAUACUGGUG matches the target *G6pc*-R83C mouse genome, containing a C83 (UGC) codon and the two synonymous variants (underlined) that had been introduced into the *G6pc*-R83C mouse genome to provide a BstX1 diagnostic restriction site.

The *G6pc* exon 2-specific dsODN sequence is TTCATAAACTTGTTCTGTTTTTTTATAGGATTCTCTTTGGACAGCGC CC**T**TACT in which some phosphorothioate bonds and 2'O-methyl bases were incorporated to increase nuclease resistance. This dsODN sequence contains a 3' intron 1 sequence including a synthetic 3' splice acceptor site, based on the analogous human *G6PC* intron sequence and the *G6pc* exon 2 sequence (underlined) that contains both the corrected R83 codon (CGC, boxed) and a synonymous variant T (bold) that disrupts the diagnostic BstX1 site. The LNP-formulated with a Cas9 mRNA:gRNA:dsODN ratio of 3:10:2 (LNP-dsODN) was

infused at 3 mg/kg into 2- and 4-week-old *G6pc*-R83C mice via the retro-orbital sinus. Age- and sex-matched wild-type (*G6pc*-R83) and heterozygote (*G6pc*-R83/C83) littermates with indistinguishable phenotype were used as the controls.

For fasting blood glucose analysis, each control or LNP-dsODN-treated mouse was transferred to a clean cage supplemented only with water. Fasting analysis was performed on blood obtained from the tip of the tail at the designated hours for as long as 24 hours of food deprivation. Blood glucose levels were measured using the HemoCue® Glucose 201 System (HemoCue America, Brea, CA). Hematoxylin and eosin (H&E) staining was performed on liver sections preserved in 10% neutral buffered formalin and Oil Red O staining was performed on cryopreserved OCT embedded liver sections following the standard procedures. The stained sections were visualized using the Imager A2m microscope with Axiocam 506 camera and the ZEN 2.6 software (Carl Zeiss, White Plains, NY).

2.3 | Phosphohydrolase assays

Liver microsome isolation and microsomal phosphohydrolase assays were performed as described previously.[9,19] In phosphohydrolase assays, reaction mixtures (50 μl) containing 50 mM sodium cacodylate buffer, pH 6.5, 2 mM EDTA, 10 mM G6P, and appropriate amounts of microsomal preparations were incubated at 30 °C for 10 min. Disrupted microsomal membranes were prepared by incubating intact membranes in 0.2% deoxycholate for 20 min at 4 °C. Non-specific phosphatase activity was estimated by pre-incubating disrupted microsomal preparations at pH 5 for 10 min at 37 °C to inactivate the acid-labile G6Pase-α. One unit of G6Pase-α activity represents one nmol G6P hydrolysis per minute per mg microsomal protein. The lower detection level of quantitation for the microsomal G6Pase-α assay is 2 units.

Enzyme histochemical analysis of G6Pase-α was performed as described previously.[9,19] Briefly, 10 μm thick liver tissue sections were incubated for 10 min at room temperature in a solution containing 40 mM Tris-maleate pH 6.5, 10 mM G6P, 300 mM sucrose, and 3.6 mM lead nitrate. After rinsing, liver sections were incubated for 2 min at room temperature in 0.09% ammonium sulfide solution and the trapped lead phosphate was visualized following conversion to the brown colored lead sulfide.

2.4 | Serum and liver metabolites measurement

To measure serum metabolites, blood was collected by intracardiac bleeding from non-fasted, anesthetized mice at sacrifice. Serum glucose, total cholesterol, and uric acid were analyzed using Glucose Liquid Stable Reagent, Cholesterol Liquid Stable Reagent, and Uric Acid Liquid Stable Reagent, respectively from ThermoFisher Scientific (Waltham, MA). Serum triglyceride was analyzed using theTriglyceride Quantification Colorimetric/Fluorometric Kit from BioVision, Inc (Milpitas, CA). Serum lactate was analyzed using the L-Lactate Assay Kit from Abcam (Boston, MA).

Liver tissues were homogenized in 5% NP-40, incubated for 5 min at 99 °C, and centrifuged to remove insoluble material. Hepatic glycogen, G6P, glucose and lactate in the deproteinized supernatants were analyzed using the Glycogen Colorimetric Assay Kit II, Glucose-6-Phosphate Colorimetric Assay Kit, Glucose Colorimetric Assay Kit II, and

Lactate Colorimetric/Fluorometric Assay Kit, respectively from BioVision, Inc. Hepatic triglycerides were isolated by homogenizing 20 mg liver tissues in 200 μl of 5% NP-40. Samples were subjected to two heating/cooling cycles of incubation for 5 min at 85 °C, followed by cooling to room temperature. Samples were then centrifuged for 15 min at 17,000 × g and triglycerides in the supernatant solutions measured using the Triglyceride Quantification Colorimetric/Fluorometric Kit from BioVision, Inc.

2.5 | Next generation sequencing

Next generation sequencing (NGS) was used to determine the percentage of cells in the liver with corrections, and insertions or deletions (indels). In brief, genomic DNA was isolated from the frozen mouse liver tissues using the Wizard Genomic DNA Purification Kit (Promega, Madison, WI, USA), then subjected to PCR to amplify a 965-nucleotide fragment harboring mouse *G6pc* exon 2 using the primer pair: forward, ACCCGATGTCAAAAGAGACAGGTG and reverse, ATCTGGATCAGGCTGCTAGGAAGG. To add specificity for mouse *G6pc*, a second PCR was performed using a nested primer pair with the following locus-specific sequence: forward, CCTTGAAACTGTGGGCTTCC, and reverse, ACTGCTTTATTATAGGCACGGAG. The 5′ end of the nested primers included either forward or reverse adaptor sequences to allow the addition of barcodes and Illumina sequencing adaptors. These adaptor sequences were: forward, 5′-TCGTCGGCAGCGTCAGATGTGTATAAGAGACAG [locus-specific sequence]; and reverse, 5′-GTCTCGTGGGCTCGGAGATGTGTATAAGAGACAG [locus-specific sequence]. The resulting amplicons were sequenced on an Illumina MiSeq using version 2 chemistry (Illumina, San Diego, CA, USA). The sequences were compiled using paired end reads with the PEAR software[28] and the percentage of each editing outcome determined. The reads consist of total insertions, unedited p.C83 pathogenic alleles, functional edited p.R83 alleles, and nonfunctional edited alleles. Functional editing represents any allele with the correcting dsODN inserted into the *G6pc* locus in the correct position and orientation, that may include indels only 5’ of the intronic insertion site. Nonfunctional alleles represent insertion of the correcting dsODN in the wrong position, or the wrong orientation, and any insertion with indels internally or at the 3’ end of the insertion site.

2.6 | Quantitative real-time RT-PCR

Total RNA was extracted from liver tissues using the TRIzol Reagent (ThermoFisher Scientific, Waltham, MA), then purified using the RNeasy Mini Kit (Qiagen, Germantown, MD). The cDNA was generated using the High-Capacity cDNA Reverse Transcription Kit (ThermoFisher Scientific). The mRNA expression was quantified by real-time RT-PCR using the TaqMan® Gene Expression Assay and Applied Biosystems QuantStudio™ 3 Real-Time PCR System (ThermoFisher Scientific). Data were normalized to Rpl19 mRNA.

2.7 | Statistical analysis

The unpaired t-test was performed using the GraphPad Prism Program, version 8 (GraphPad Software, CA). Values were considered statistically significant at $p < 0.05$.

3 | RESULTS

3.1 | The dsODN insertional strategy

The *G6pc*-R83C mice, carrying the pathogenic p.R83C variant in exon 2 of the *G6pc* gene, manifest impaired glucose homeostasis characterized by fasting hypoglycemia, hepatomegaly, nephromegaly, hyperlipidemia, hyperuricemia, and growth retardation.[19] Using the *G6pc*-R83C mice, we evaluated the efficacy of the CRISPR/Cas9-based short dsODN insertional strategy[25] to correct the p.R83C mutation. The strategy introduces a DSB in the *G6pc* gene ~7bp downstream of the *G6pc* p.R83C codon, splitting exon 2 into a 5′ sequence and 3′ sequence (Figure 1). The dsODN can then insert into the split exon by NHEJ to introduce a synthetic 3′ acceptor splice site and sequences that reconstitute exon 2 with the correct R83 codon. This outcome results in a genome that contains the truncated 5′ exon 2 of *G6pc*, followed by the synthetic 3′ splice acceptor site, and a corrected version of *G6pc* exon 2. (Figure 1). When transcribed, the resulting primary *G6pc* transcript contains two relatively close 3′ acceptor splice sites for exon 2 and a single 5′ donor splice site. Based on prediction algorithms, such as Spliceator,[29] we predicted splicing would preferentially use the synthetic acceptor splice site, leading to a *G6pc* mRNA containing wild-type exon 2 encoding wild-type G6Pase-α (G6PC) protein (Figure 1). During NHEJ, the dsODN can also insert into the *G6pc* locus in the reverse orientation, which would not lead to a productive *G6pc* transcript. Similarly, any variation in the site of genome cleavage and creation of any indels could lead to out of frame insertions and non-productive *G6pc* transcripts.[25] Our previous studies[9,10] have shown that restoring hepatic G6Pase-α activity to ≥3% of normal hepatic G6Pase-α activity is sufficient to normalize metabolism.

3.2 | The dsODN insertional strategy corrects metabolic manifestations of the *G6pc*-R83C mice

We evaluated the efficacy of the CRISPR/Cas9-based dsODN insertional strategy to correct the pathogenic p.R83C mutation in the *G6pc*-R83C mice using either one dose of LNP-dsODN at age 4 weeks (dsODN-1D mice) or two doses of LNP-dsODN, one at age 2 weeks and the second at age 4 weeks (dsODN-2D mice). Both were infused via the retro-orbital sinus and glucose therapy was terminated immediately following infusion. The 4-week and 6-week survival rates of the *G6pc*-R83C mice were ~15% and 0%, respectively.[19]

To evaluate the efficacy of LNP-dsODN and a time point where liver growth had slowed more, we first treated 4-week-old *G6pc*-R83C mice with one dose of LNP-dsODN. Out of the seven dsODN-1D mice, six grew to adulthood with an 8-week survival rate of 86%. Phenotypic correction in the dsODN-1D mice was assessed at age 8 weeks. Liver microsomal G6Pase-α enzyme activities in 8-week-old control mice averaged 202.9 ± 17.2 units, representing 100% of normal hepatic G6Pase-α activity, while in 8-week-old dsODN-1D mice (n = 6), the activity averaged 7.3 ± 1.6 units, representing 3.6 ± 0.8% of normal hepatic G6Pase-α activity (Figure 2A). NGS analysis of liver tissues of the 8-week-old dsODN-1D (n = 6) mice showed that hepatic G6Pase-α activity restored correlated linearly with functional editing (C83 to R83), non-functional editing, and total indels in the *G6pc* locus (Figure 2B).

The hallmark of GSD-Ia is fasting hypoglycemia.[1–3] While the untreated *G6pc*-R83C mice could not tolerate even a short fast, the dsODN-1D mice could sustain 6 hours of fasting (Figure 2C). Compared to the controls, the dsODN-1D mice displayed reduced serum levels of glucose but normal serum levels of cholesterol, triglyceride, lactic acid, and uric acid (Figure 2D).

The 8-week-old dsODN-1D mice remained growth retarded, and their body weight (BW) values at 19.1 ± 1.2 g were 66% of their age-matched control mice at 28.9 ± 1.4 g (Figure 2E). The body mass index (BMI) values of the dsODN-1D mice were significantly lower than that of their control littermates (Figure 2E), indicating that the dsODN-1D mice were considerably leaner. The dsODN-1D mice continued manifesting hepatomegaly with a liver weight (LW)/BW value of 9.8 ± 0.7% and nephromegaly (Figure 2E), consistent with our previous studies.[9,19]

Compared to the controls, the 8-week-old dsODN-1D mice had reduced hepatic levels of glucose but increased hepatic levels of glycogen, triglyceride, lactate, and G6P (Figure 2F). Hepatic levels of glycogen in 8-week-old control and dsODN-1D mice averaged 181.0 ± 36.4 and 630.4 ± 65.8 nmol/mg, respectively, indicating a 4.5-fold increase in glycogen in the dsODN-1D mice. Hepatic levels of triglyceride in 8-week-old control and dsODN-1D mice averaged 84.9 ± 17.9 and 367.1 ± 50.5 nmol/mg, respectively, indicating a 4.3-fold increase in triglyceride in the dsODN-1D mice (Figure 2F).

Due to the low (15%) survival rate of the *G6pc*-R83C mice to age 4 weeks, we also tested our therapy by treating *G6pc*-R83C mice with two doses of LNP-dsODN, one at age 2 weeks, the other at age 4 weeks. This strategy successfully supported the growth of all eight dsODN-2D mice to adulthood with a 16-week survival rate of 100%.

Liver microsomal G6Pase-α activity in 16-week-old control mice (n = 10) averaged 178.1 ± 17.8 units, representing 100% of normal hepatic G6Pase-α activity (Figure 3A). Liver microsomal G6Pase-α activity in 16-week-old dsODN-2D mice (n = 8) averaged 7.1 ± 0.7 units (Figure 2A), representing 4.0 ± 0.4% of normal hepatic G6Pase-α activity. NGS analysis of liver tissues of the 8-week-old dsODN-2D (n = 8) mice showed that hepatic G6Pase-α activity restored correlated linearly with functional editing (C83 to R83), non-functional editing, and total indels in the *G6pc* locus (Figure 3B).

The 16-week-old dsODN-2D mice could survive 24 hours of fasting (Figure 3C). When not fasting, the treated mice displayed normal serum levels of triglyceride, cholesterol, lactic acid, and uric acid although their serum glucose levels remained lower than those of the control mice (Figure 3D).

At age 16 weeks, the BW values of the dsODN-2D mice averaged 72% of their age-matched control mice and their BMI values were significantly lower than those of the controls (Figure 3E), again suggesting that the dsODN-2D mice were leaner. These results are consistent with our studies of both *G6pc*−/− mice treated by rAAV-G6PC-mediated gene augmentation therapy,[9] and *G6pc*-R83C neonates that were edited using HDR.[19] The dsODN-2D mice continued manifesting hepatomegaly and nephromegaly (Figure 3E). However, the LW/BW

values of the 16-week-old dsODN-2D mice at 7.9 ± 0.5% were significantly lower than the LW/BW values of the 8-week-old dsODN-1D mice at 9.8 ± 0.7% were (Figure 2E).

Compared to the controls, intracellular hepatic glucose levels in the 16-week-old dsODN-2D mice remained lower, and the dsODN-2D mice continued displaying increased hepatic levels of glycogen, lactate, and G6P (Figure 3F). Hepatic levels of glycogen in 16-week-old control and dsODN-2D mice averaged 246.5 ± 39.5 and 371.0 ± 34.4 nmol/mg, respectively, indicating a 1.5-fold increase in glycogen in the dsODN-2D mice. The increase in hepatic glycogen levels in the 16-week-old dsODN-2D mice was significantly smaller than the 4.5-fold increase in glycogen levels in the 8-week-old dsODN-1D mice (Figure 2F). Significantly, hepatic levels of triglyceride in 16-week-old control and dsODN-2D mice averaged 155.2 ± 45.8 and 175.0 ± 73.9 nmol/mg, respectively, suggesting near complete normalization of neutral fat in the dsDON-2D mice (Figure 3F). This contrasts with the 4.3-fold increase in triglyceride in the dsODN-1D mice (Figure 2F).

The reasons responsible for the apparent metabolic improvement in the 16-week-old dsODN-2D mice compared to the 8-week-old dsODN-1D mice are twofold. Firstly, double doses verse a single dose of LNP-dsODN. Secondly, the differing length of therapy, namely 12 weeks for the dsODN-2D mice versus 4 weeks for the dsODN-1D mice. Consistent with this we have previously shown that in the neonatal *G6pc*-R83C mice edited using HDR,[19] the LW/BW ratio decreased with the length of therapy for at least the first 16 weeks of therapy.

3.3 | Biochemical phenotype of the dsODN mice

Enzyme histochemical analysis showed that G6Pase-α in 8- and 16-week-old control mice was distributed throughout the liver with significantly higher levels in proximity to blood vessels (Figure 4A). G6Pase-α in 8-week-old dsODN-1D and 16-week-old dsODN-2D mice was also distributed throughout the liver but with foci containing markedly higher levels of enzymatic activity in proximity to blood vessels and a substantial proportion of hepatocytes further from blood vessels harboring little or no G6Pase-α activity (Figure 4A), consistent with the findings of rAAV-G6PC-mediated gene augmentation therapy[9] and the neonatal *G6pc*-R83C mice edited using HDR.[19]

H&E staining showed both the 8-week-old dsODN-1D and 16-week-old dsODN-2D mice exhibited no hepatic histological abnormalities except their hepatocytes displayed a diffuse mosaic pattern consistent with increased glycogen accumulation (Figure 4B). Oil red O staining showed that the 8-week-old dsODN-1D mice displayed increased neutral fat storage while the 16-week-old dsODN-2D mice displayed normalized neutral fat storage (Figure 4C), in agreement with their hepatic triglyceride levels.

Glucose homeostasis is maintained by the coupled action of the G6Pase-α/G6P transporter (G6PT) complex.[1–3] In previous studies[9,19] we have shown that the reduced hepatic G6Pase-α activity can be offset by an increase in hepatic G6PT expression. Consistent with this, the hepatic *G6pt* mRNA levels in the dsODN-1D mice were 1.7-fold over that of the controls (Figure 4D).

4 | DISCUSSION

GSD-Ia is a rare, potentially neonatal lethal disease caused by pathogenic variants in the *G6PC* gene that encodes the enzyme G6Pase-α.[1–3,7] Loss of G6Pase-α enzyme activity in the gluconeogenic organs leads to impaired blood glucose homeostasis characterized by fasting hypoglycemia, hepatomegaly, nephromegaly, hyperlipidemia, hyperuricemia, lactic acidemia, and growth retardation.[1–3,7] G6Pase-α is an endoplasmic reticulum transmembrane protein, and as such is refractory to traditional enzyme replacement therapies. We have demonstrated, in preclinical studies, that rAAV-G6PC-mediated gene augmentation therapy for GSD-Ia is safe and effective,[8–10] and this therapy is now entering phase III clinical trials (NCT05139316). Due to the mitotic growth of the human liver during childhood, intervention using an episomal rAAV gene augmentation therapy may be limited by the age at which effective intervention can be initiated. Furthermore, the long-term clinical durability of episomal rAAV expression, which must last the full lifetime of the patient, is unclear.[11] One interpretation of recent studies on the rate of physiological cell replacement in the mature liver could be that episomal gene augmentation might require re-administration to maintain efficacy.[12] As a more permanent alternative therapy, we are exploring genome editing. In a previous preclinical study, we generated *G6pc*-R83C mice carrying the G6PC-p.R83C variant in exon 2 of the *G6pc* gene and showed that the *G6pc*-R83C mice exhibit the symptoms of impaired glucose homeostasis mimicking human GSD-Ia.[19] We further showed that the abnormal metabolic phenotype of the *G6pc*-R83C mice could be corrected using a CRISPR/Cas9-mediated HDR editing strategy, delivered using dual AAV vectors, to treat neonatal mice.[19] More recently, Arnson et al. showed that fasting hypoglycemia and the survival of two GSD-Ia puppies carrying the G6PC-p.M121I pathogenic variant could be improved using a similar CRISPR/Cas9-based HDR editing strategy, delivered using dual AAV vectors.[30] However, interpretation of the data was complicated by the repeat administrations of rAAV-mediated gene therapy to each puppy at ages 2–3 months.[30] Intervention at a slightly older age, effective in a larger, less rapidly growing liver would be attractive.

In the current study we explore the use a CRISPR/Cas-9-based editing strategy that uses the NHEJ repair mechanism which is effective in both dividing and non-dividing cells.[22–24] The *G6pc*-R83C mice exhibit all aspects of the human GSD-Ia disease,[19] and even in the presence of glucose therapy, survival at age 4 weeks is ~15% and no mice survive to 6 weeks. The *G6pc*-R83C mice were treated with either signal dose (dsODN-1D) or two doses (dsODN-2D) of LNP-dsODN. While the dsODN-1D mice had an 8-week survival rate of 86%, the dsODN-2D had a 16-week survival rate of 100%. The dsODN-1D and dsODN-2D mice expressed 3.6% to 4.0% of normal hepatic G6Pase-α activity, levels previously shown to be therapeutic.[9,10,19] We showed that both dsODN-1D and dsODN-2D mice could sustain fasting at least 6 hours, with the 16-week-old dsODN-2D mice sustaining a 24 hour fast. The viability and glucose control observed for both dsODN-1D and dsODN-2D mice strongly suggest that they may survive long-term and maintain glucose homeostasis. The dsODN-treated mice displayed an improved metabolic phenotype similar to that observed in the neonatal *G6pc*-R83C mice edited by CRISPR/Cas9-mediated HDR[19] and the preclinical

studies of rAAV-G6PC-mediated gene augmentation therapy, that has recently entered phase III clinical trials (NCT05139316).

We have previously shown that in rAAV-G6PC-mediated gene augmentation therapy, the treated *G6pc*−/− mice expressing ≥3% of normal hepatic G6Pase-α activity maintain glucose homeostasis and have no HCA/HCC,[9,10] which is a severe long-term complication of GSD-Ia.[1–3,7] However, mice harboring less than 2% of normal hepatic G6Pase-α activity are at an increased risk for tumor development,[10] defining a baseline for effective long-term gene therapy. Longer-term studies of ~12-month-old dsODN-treated mice will be required to confirm the durability of the edited cell population and determine if the edited mice can survive long-term, and maintain glucose homeostasis without developing hepatic tumors.

Blood glucose homeostasis is maintained by the G6Pase-α/G6PT complex.[1–3] The rate-limiting step in the G6Pase-α/G6PT complex is the G6PT-mediated microsomal uptake of G6P which is co-dependent upon G6Pase-α activity.[31] We have shown previously that in the presence of a reduced G6Pase-α activity in mice, there is a feedback mechanism that increases substrate availability for G6Pase-α by increasing G6PT expression.[9,10,19] As expected, the dsODN-1D mice expressing 3.6% of normal hepatic G6Pase-α activity also exhibited elevated hepatic *G6pt* expression.

The NHEJ-mediated dsODN insertional strategy we explored could lead to at least four outcomes[25]: 1) insertion of the correcting dsODN in the correct orientation in the absence of indels at the site of genome cleavage; 2) insertion of the correcting dsODN in the correct orientation in the presence of indels at either or both junctions of the insertion; 3) insertion of the correcting dsODN in the reverse orientation in the absence of indels; and 4) insertion of the correcting dsODN in the reverse orientation in the presence of indels. Outcome (1) and outcome (2) with small indels restricted to being adjacent to the introduced synthetic 3′ acceptor splice site can yield a functional *G6pc* mRNA and protein, while the other outcomes of (2) or (3) or (4) will be non-functional. Other non-productive outcomes of this strategy will, of course, include failure to cleave the target site; cleavage and re-ligation, without insertion, with or without indels; and any transcripts that continue to use the original intron1-exon 2 splice acceptor site.

The potential advantages of the current strategy are: 1) introducing a permanent somatic correction of the *G6pc* gene that is robust to liver renewal throughout life; 2) overcoming age-restrictions that may emerge for rAAV-mediated gene augmentation therapy; 3) avoiding expensive rAAV manufacturing; 4) avoiding rAAV-related inflammation and host immune responses; and 5) avoiding potential complications from longer-term expression of Cas9 and the editing reagents mediated by AAV delivery.

The present study was designed as a functional proof-of-concept to determine if the GSD-Ia mouse *G6pc* locus was sufficiently accessible to gene editing to establish viable glucose homeostasis. While the outcome was successful, the editing efficiency was not as high above the functional cut-off as we would need for translational studies into humans. As such, our primary ongoing interest is improving the efficiency of editing the *G6pc* locus, before evaluating and mitigating off-target editing. Consistent with this we have similarly not

evaluated long term implications such as immune responses or toxicity to the LNP-dsODN reagent.

In summary, we have provided an initial proof of concept study that a CRISPR/Cas9-based dsODN insertional strategy exploiting the NHEJ repair mechanism may be worthy of further development. When applied to 2- to 4-week-old *G6pc*-R83C mice, this *in vivo* therapy can effectively correct the pathogenic G6PC-p.R83C variant in the liver of GSD-Ia mice and improve their metabolic abnormalities for at least 16 weeks. The transient LNP-mediated delivery of editing reagents to the liver was effective and offers the potential to reduce multiple risks associated with viral delivery of editing reagents. These outcomes suggest further exploration of a permanent genome edit to correct prevalent pathogenic *G6PC* variants in GSD-Ia is warranted as a viable alternative therapeutic approach to rAAV-G6PC-mediated gene augmentation therapy.

ACKNOWLEDGEMENT

We thank CRISPR Therapeutics, Inc. for production of the LNP-dsODN reagent. We also thank Fabio R. Faucz, James R. Iben, and Tianwei Li at Molecular Genomics Core, *Eunice Kennedy Shriver* National Institute of Child Health and Human Development, National Institutes of Health for NGS analysis.

FUNDING INFORMATION

This work was supported by the Intramural Research Program of the *Eunice Kennedy Shriver* National Institute of Child Health and Human Development, National Institutes of Health and The Children's Fund for Glycogen Storage Disease Research.

NICHD - HD000912-38 (https://intramural.nih.gov/search/searchview.taf?ipid=100503&ts=1513174914).

DATA AVAILABILITY STATEMENT

The data that support the findings of this study are available from the corresponding author upon reasonable request.

LIST OF ABBREVIATIONS

AAV	adeno-associated virus
BMI	body mass index
BW	body weight
DSB	DNA double-strand break
G6P	glucose-6-phosphate
G6Pase-α	glucose-6-phosphatase-α
G6PT	glucose-6-phosphate transporter
GSD-Ia	glycogen storage disease type Ia
HCA	hepatocellular adenoma
HCC	hepatocellular carcinoma

HDR	homology-directed repair
H&E	hematoxylin and eosin
Indels	insertions or deletions
LW	liver weight
NHEJ	non-homologous end joining
gRNA	single guide RNA

REFERENCES

1. Chou JY, Matern D, Mansfield BC, Chen YT. Type I glycogen storage diseases: disorders of the glucose-6-phosphatase complex. Curr Mol Med. 2002;2(2):121–143. [PubMed: 11949931]
2. Chou JY, Jun HS, Mansfield BC. Glycogen storage disease type I and G6Pase-beta deficiency: etiology and therapy. Nat Rev Endocrinol. 2010;6(12):676–688. [PubMed: 20975743]
3. Chou JY, Jun HS, Mansfield BC. Type I glycogen storage diseases: Disorders of the glucose-6-phosphatase/glucose-6-phosphate transporter complexes. J Inherit Metab Dis. 2015;38(3):511–519. [PubMed: 25288127]
4. Greene HL, Slonim AE, O'Neill JA Jr, Burr IM. Continuous nocturnal intragastric feeding for management of type 1 glycogen-storage disease. N Engl J Med. 1976;294(8):423–425. [PubMed: 813144]
5. Chen YT, Cornblath M, Sidbury JB. Cornstarch therapy in type I glycogen storage disease. N Engl J Med. 1984;310(3):171–175. [PubMed: 6581385]
6. Ross KM, Ferrecchia IA, Dahlberg KR, Dambska M, Ryan PT, Weinstein DA. Dietary management of the glycogen storage Diseases: evolution of treatment and ongoing controversies. Adv Nutr. 2020;11(2):439–446. [PubMed: 31665208]
7. Kishnani PS, Austin SL, Abdenur JE, et al. Diagnosis and management of glycogen storage disease type I: a practice guideline of the American College of Medical Genetics and Genomics. Genet Med. 2014;16(11):e1. [PubMed: 25356975]
8. Yiu WH, Lee YM, Peng WT, et al. Complete normalization of hepatic G6PC deficiency in murine glycogen storage disease type Ia using gene therapy. Mol Ther. 2010;18(6):1076–1084. [PubMed: 20389290]
9. Lee YM, Jun HS, Pan CJ, et al. Prevention of hepatocellular adenoma and correction of metabolic abnormalities in murine glycogen storage disease type Ia by gene therapy. Hepatology. 2012;56(5):1719–1729. [PubMed: 22422504]
10. Kim GY, Lee YM, Kwon JH, et al. Glycogen storage disease type Ia mice with less than 2% of normal hepatic glucose-6-phosphatase-α activity restored are at risk of developing hepatic tumors. Mol Genet Metab. 2017;120(3):229–234. [PubMed: 28096054]
11. Nathwani AC, McIntosh J, Sheridan R. Liver Gene Therapy. Hum Gene Ther. 2022;33(17–18):879–888. [PubMed: 36082993]
12. Heinke P, Rost F, Rode J, et al. Diploid hepatocytes drive physiological liver renewal in adult humans. Cell Syst. 2022;13(6):499–507.e12. [PubMed: 35649419]
13. Ran FA, Hsu PD, Lin CY, et al. Double nicking by RNA-guided CRISPR Cas9 for enhanced genome editing specificity. Cell. 2013;154(6):1380–1389. [PubMed: 23992846]
14. Yang Y, Wang L, Bell P, et al. A dual AAV system enables the Cas9-mediated correction of a metabolic liver disease in newborn mice. Nat Biotechnol. 2016;34(3):334–338. [PubMed: 26829317]
15. Pankowicz FP, Jarrett KE, Lagor WR, Bissig KD. CRISPR/Cas9: at the cutting edge of hepatology. Gut. 2017;66(7):1329–1340. [PubMed: 28487442]
16. Schneller JL, Lee CM, Bao G, Venditti CP. Genome editing for inborn errors of metabolism: advancing towards the clinic. BMC Med. 2017;15(1):43. [PubMed: 28238287]

17. Pickar-Oliver A, Gersbach CA. The next generation of CRISPR-Cas technologies and applications. Nat Rev Mol Cell Biol. 2019;20(8):490–507. [PubMed: 31147612]
18. Asmamaw M, Zawdie B. Mechanism and Applications of CRISPR/Cas-9-Mediated Genome Editing. Biologics. 2021;15:353–361. [PubMed: 34456559]
19. Arnaoutova I, Zhang L, Chen HD, Mansfield BC, Chou JY. Correction of metabolic abnormalities in a mouse model of glycogen storage disease type Ia by CRISPR/Cas9-based gene editing. Mol Ther. 2021;29(4):1602–1610. [PubMed: 33359667]
20. Chou JY, Mansfield BC. Mutations in the glucose-6-phosphatase-α (G6PC) gene that cause type Ia glycogen storage disease. Hum Mutat. 2008;29(7):921–930. [PubMed: 18449899]
21. Lei KJ, Shelly LL, Pan CJ, Liu J-L, Chou JY. Structure-function analysis of human glucose-6-phosphatase, the enzyme deficient in glycogen storage disease type 1a. J Biol Chem. 1995;270(20):11882–11886. [PubMed: 7744838]
22. Mao Z, Bozzella M, Seluanov A, Gorbunova V. Comparison of nonhomologous end joining and homologous recombination in human cells. DNA Repair (Amst). 2008;7(10):1765–1771. [PubMed: 18675941]
23. Lieber MR. The mechanism of double-strand DNA break repair by the nonhomologous DNA end-joining pathway. Annu Rev Biochem. 2010; 79: 181–211. [PubMed: 20192759]
24. Zhao B, Rothenberg E, Ramsden DA, Lieber MR. The molecular basis and disease relevance of non-homologous DNA end joining. Nat Rev Mol Cell Biol. 2020;21(12):765–781. [PubMed: 33077885]
25. Hart C, Beaudry K, Bayles T, et al. Insertion of short double-stranded oligonucleotides using CRISPR/CAS9 as a therapeutic approach for glycogen storage disease type 1a. American Society of Gene & Cell Therapy. 2020; Abstract.
26. Samaridou E, Heyes J, Lutwyche P. Lipid nanoparticles for nucleic acid delivery: Current perspectives. Adv Drug Deliv Rev. 2020;154–155:37–63.
27. Böttger R, Pauli G, Chao PH, Al Fayez N, Hohenwarter L, SD Li. Lipid-based nanoparticle technologies for liver targeting. Adv Drug Deliv Rev. 2020;154–155:79–101.
28. Zhang J, Kobert K, Flouri T, Stamatakis A. PEAR: a fast and accurate Illumina Paired-End reAd mergeR. Bioinformatics 2014;30(5); 614–620. [PubMed: 24142950]
29. Scalzitti N, Kress A, Orhand R, Weber T, Moulinier L, Jeannin-Girardon A, Collet P, Poch O, Thompson JD. Spliceator: multi-species splice site prediction using convolutional neural networks. BMC Bioinformatics. 2021;22(1):561. [PubMed: 34814826]
30. Arnson B, Kang HR, Brooks ED, et al. Genome editing using Staphylococcus aureus Cas9 in a canine model of glycogen storage disease Ia. Mol Ther Methods Clin Dev. 2023;29:108–119. [PubMed: 37021039]
31. Lei KJ, Chen H, Pan CJ, et al. Glucose-6-phosphatase dependent substrate transport in the glycogen storage disease type-1a mouse. Nat Genet. 1996;13(2):203–209. [PubMed: 8640227]

Synopsis

Using *G6pc*-R83C mice, a model for GSD-Ia which carries a prevalent human *G6PC* pathogenic variant, we show that a CRISPR/Cas9-based dsODN insertional strategy corrects the hallmark metabolic abnormalities of disease, offering a non-inheritable, potentially permanent correction of the GSD-Ia phenotype.

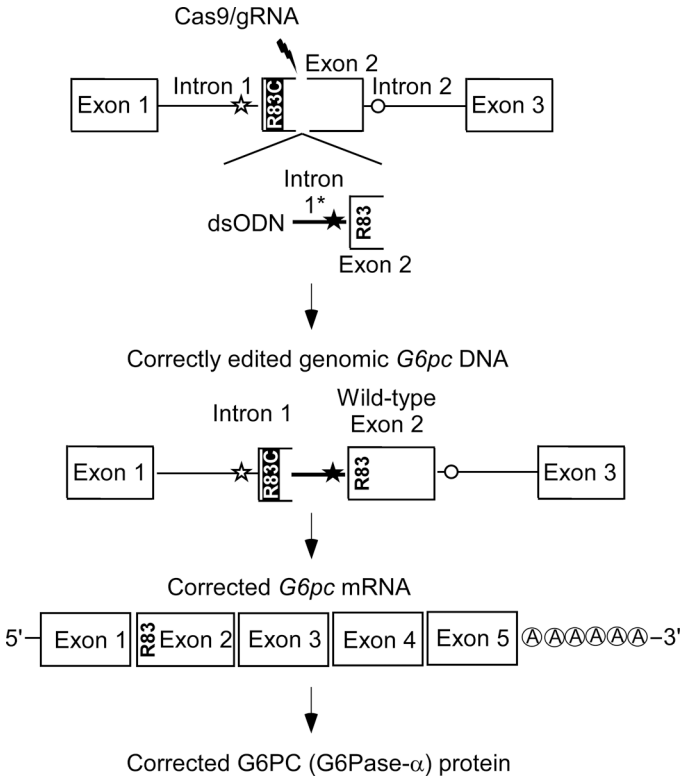

Figure 1. The dsODN insertional strategy.

Exons 1, 2, and 3 and the associated introns 1 and 2 of mouse genomic *G6pc* gene carrying the p.R83C pathogenic variant that causes GSD-Ia are depicted (not to scale). The original 3′ acceptor splice (☆) and 5′ donor splice (O) sites are shown. The gRNA directs Cas9 to create a DSB in exon 2 of the *G6pc* gene ~7 bp downstream of the p.R83C codon, splitting exon 2 into a 5′ sequence and 3′ sequence. The NHEJ-mediated insertion of the correcting dsODN in the appropriate orientation can introduce a synthetic 3′ acceptor splice site (★) and recreate the correct *G6pc* exon 2 with wild-type (p.R83) protein coding sequence. This creates two 3′ acceptor splice sites in close proximity. Algorithms, such as Spliceator,[29] predict that the synthetic 3′ acceptor splice site will be preferentially used in the primary RNA transcript resulting in a wild-type *G6pc* mRNA that encodes a wild-type (p.R83) G6Pase-α (G6PC) protein. Indels at the site of Cas9 cleavage and insertion of the dsODN in the opposite orientation to that shown can result in non-productive *G6pc* transcripts.[25]

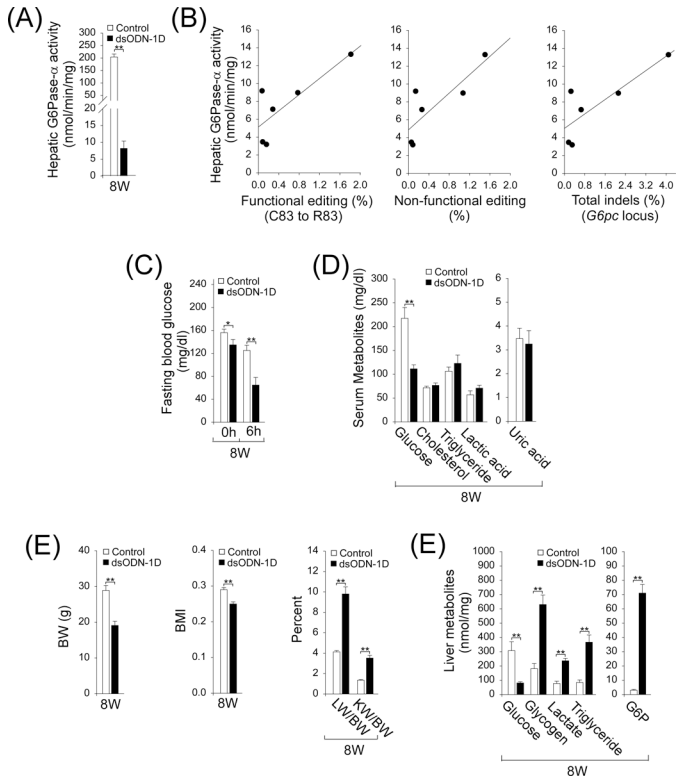

Figure 2. Phenotypic analysis of the 8-week-old dsODN-1D mice

The *G6pc*-R83 and *G6pc*-R83/R83C mice display a similar phenotype were used as the control mice. The dsODN-1D mice were transfused with the LNP-dsODN editing reagents at 4 weeks of age. Biochemical analysis was conducted in 8-week-old control (n = 8) and dsODN-1D (n = 6) mice. (A) Liver microsomal G6Pase-α activity. (B) Restoration of hepatic G6Pase-α activity as a function of functional editing (C83 to R83), non-functional editing, and total indels in the *G6pc* locus estimated by NGS of PCR amplicons in the liver tissues of the dsODN-1D mice. (C) Blood glucose levels in non-fasted (zero hour, 0h) and following 6 hours (6h) of fast. (D) Serum glucose, cholesterol, triglyceride, lactate, and uric acid levels in mice not subjected to fasting. (E) Values of body weight (BW); body mass index (BMI); percent of liver weight (LW) to BW; and percent of kidney weight (KW) to BW. (F) Hepatic levels of glucose, glycogen, lactate, triglyceride, and G6P. Data represent the mean ± SEM. *$p < 0.05$, **$p < 0.005$.

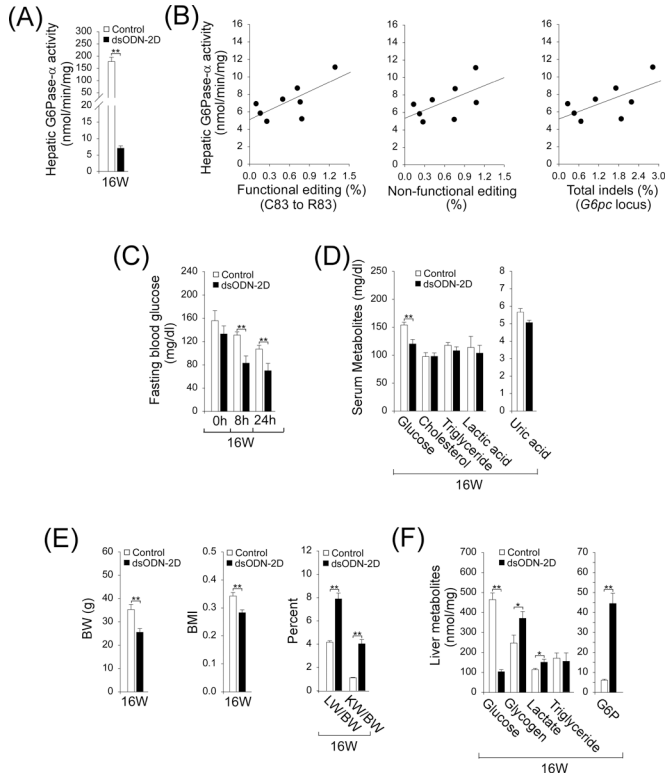

Figure 3. Phenotypic analysis of the 16-week-old dsODN-2D mice

The *G6pc*-R83 and *G6pc*-R83/R83C mice display a similar phenotype were used as the control mice. The dsODN-2D mice were transfused with the LNP-dsODN editing reagents at both 2 and 4 weeks of age. Biochemical analysis was conducted in 16-week-old control (n = 10) and dsODN-2D (n = 8) mice. (A) Liver microsomal G6Pase-α activity. (B) Restoration of hepatic G6Pase-α activity as a function of functional editing (C83 to R83), non-functional editing, and total indels in the *G6pc* locus estimated by NGS of PCR amplicons in the liver tissues of the dsODN-2D mice. (C) Blood glucose levels in non-fasted (zero hour, 0h) and following 8 hours (8h) and 24 hours (24h) of fast. (D) Serum glucose, cholesterol, triglyceride, lactate, and uric acid levels in mice not subjected to fasting. (E) Values of body weight (BW); body mass index (BMI); percent of liver weight (LW) to BW; and percent of kidney weight (KW) to BW. (F) Hepatic levels of glucose, glycogen, lactate, triglyceride, and G6P. Data represent the mean ± SEM. *$p < 0.05$, **$p < 0.005$.

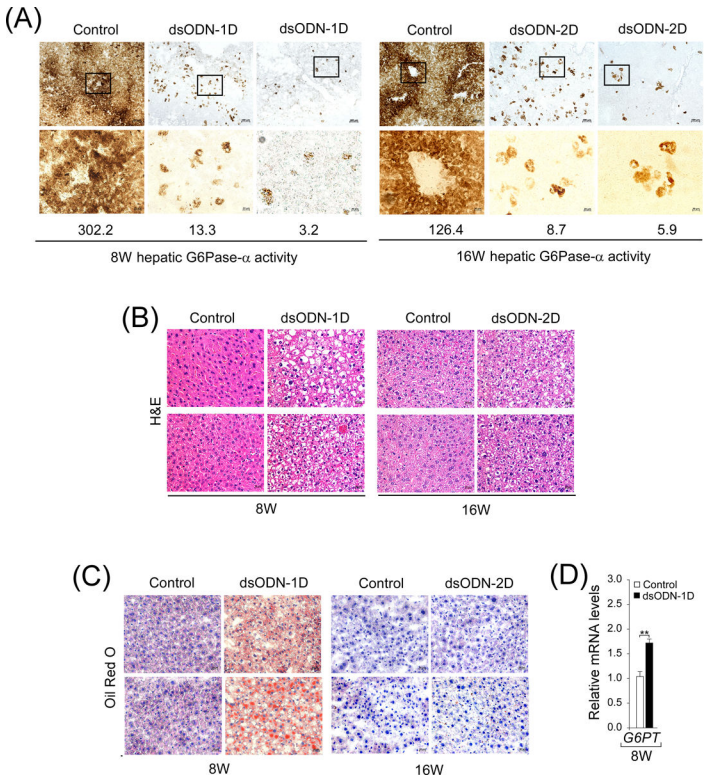

Figure 4. Biochemical analysis of dsODN-1D and dsODN-2D mice

The *G6pc*-R83 and *G6pc*-R83/R83C mice displaying a similar phenotype were used as the control mice. (A) Histochemical analysis of hepatic G6Pase-α activity. Each image represents an individual mouse. Upper, scale bar 100 μm; Bottom, scale bar 20 μm. The numbers represent hepatic G6Pase-α activity expressed in the mice. (B) H&E-stained liver sections in dsODN-1D and dsODN-2D mice and their respective control mice. Each plate represents an individual mouse. Scale bar = 20 μm. (C) Oil Red O-stained liver sections in dsODN-1D and dsODN-2D mice and their respective control mice. Each plate represents an individual mouse. Scale bar = 20 μm. (D) Hepatic levels of *G6pt* transcript. Data represent the mean ± SEM. *$p < 0.05$, **$p < 0.005$.